

Supporting Information

Corrosion-engineered transition metal multi-anionic interface for efficient electrocatalysis toward overall water splitting

Qiaolin Guo^a, Xiang Liu^a, Changwang Ke^a, Weiping Xiao^{a,b*}, Xiaofei Yang^{a*}

a. College of Science, Institute of Materials Physics and Chemistry, Nanjing Forestry University, Nanjing 210037, China

b. Key Laboratory of Advanced Energy Materials Chemistry (Ministry of Education), College of Chemistry, Nankai University, Tianjin 300071, China

*Corresponding author

E-mail address: wpxiao@njfu.edu.cn; xiaofei.yang@njfu.edu.cn

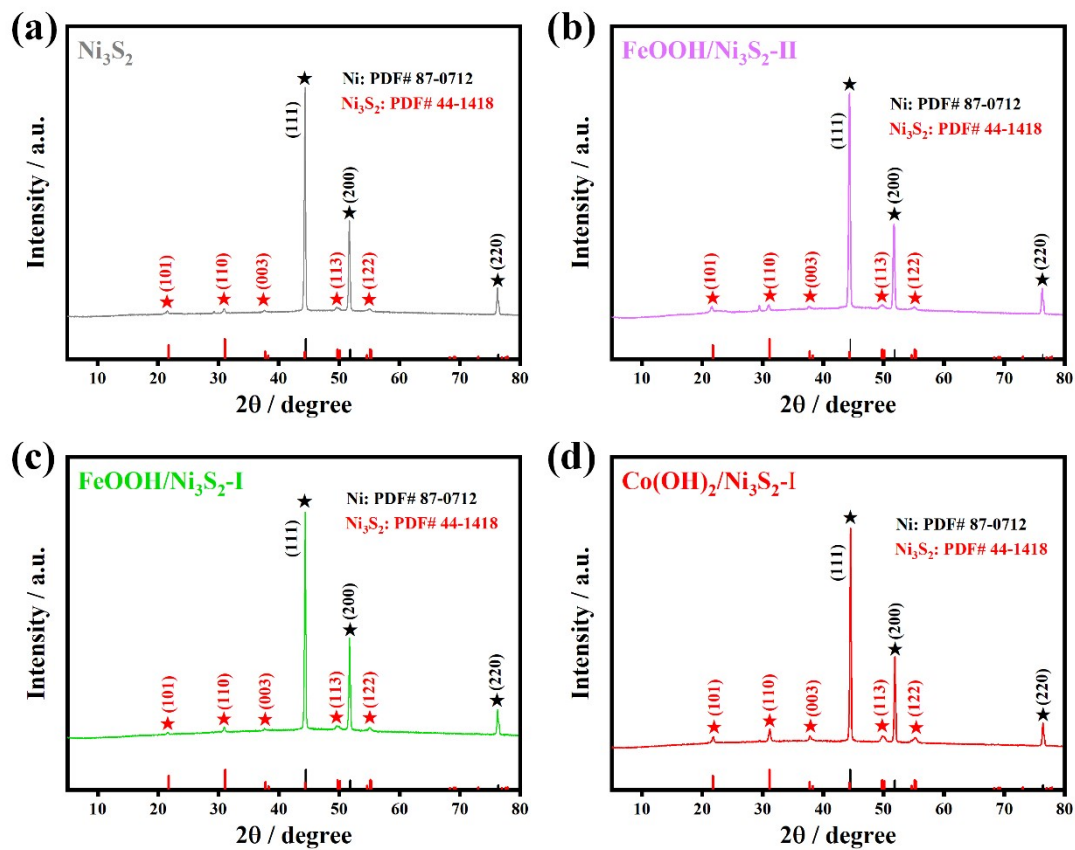


Figure S1. XRD patterns of samples: (a) Ni_3S_2 , (b) $\text{FeOOH}/\text{Ni}_3\text{S}_2\text{-II}$, (c) $\text{FeOOH}/\text{Ni}_3\text{S}_2\text{-I}$, (d) $\text{Co(OH)}_2/\text{Ni}_3\text{S}_2\text{-I}$.

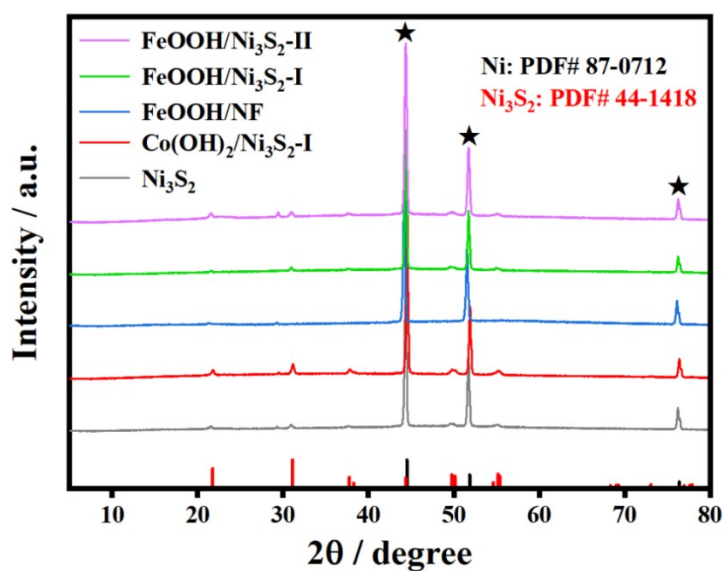


Figure S2. XRD patterns of samples $\text{FeOOH}/\text{Ni}_3\text{S}_2\text{-II}$, $\text{FeOOH}/\text{Ni}_3\text{S}_2\text{-I}$, FeOOH/NF , $\text{Co(OH)}_2/\text{Ni}_3\text{S}_2\text{-I}$ and Ni_3S_2 .

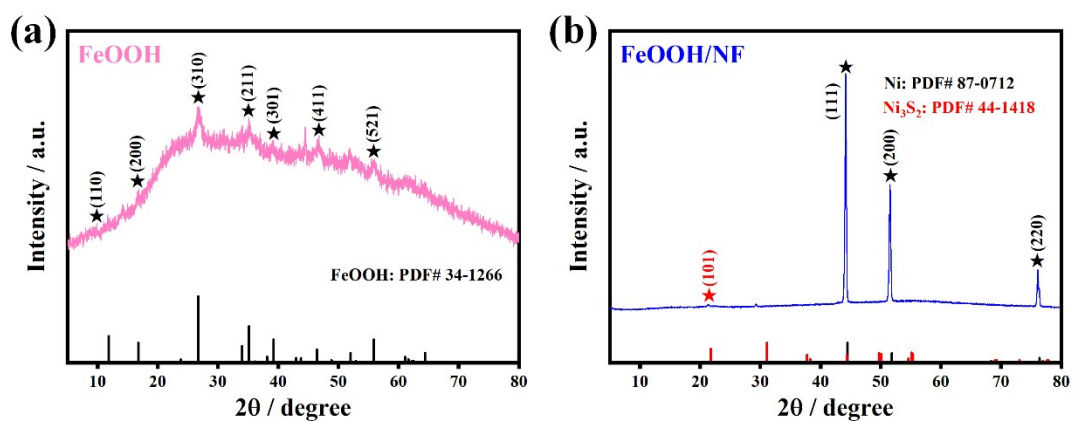


Figure S3. XRD patterns: (a) the precipitation of FeOOH was collected during the preparation process, and (b) FeOOH/NF.

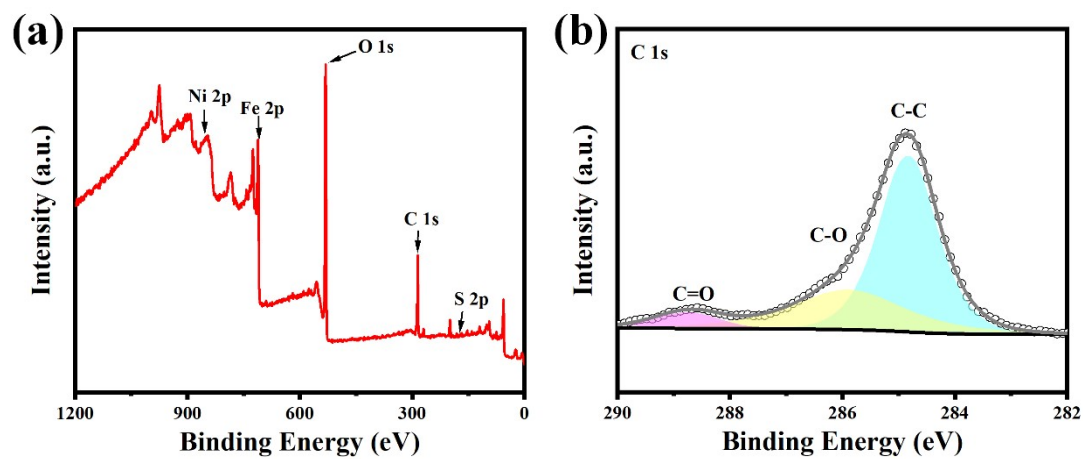


Figure S4. The X-ray photoelectron spectroscopy of FeOOH/ Ni_3S_2 -II: (a) The XPS survey spectrum, (b) High-resolution XPS spectrum of C 1s.

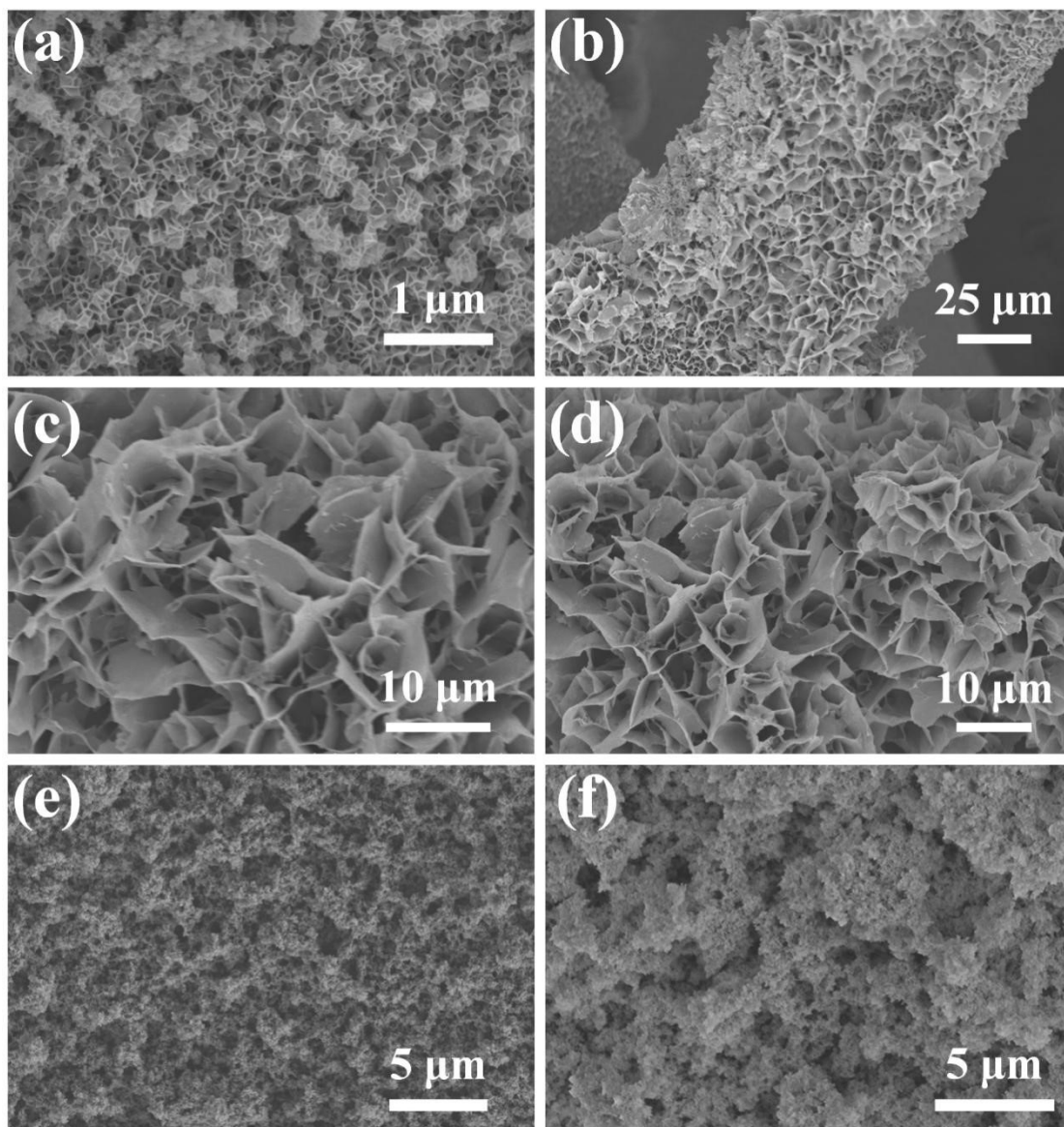


Figure S5. SEM images: (a) FeOOH/Ni₃S₂-II, (b-d) FeOOH/Ni₃S₂-I, (e, f) FeOOH.

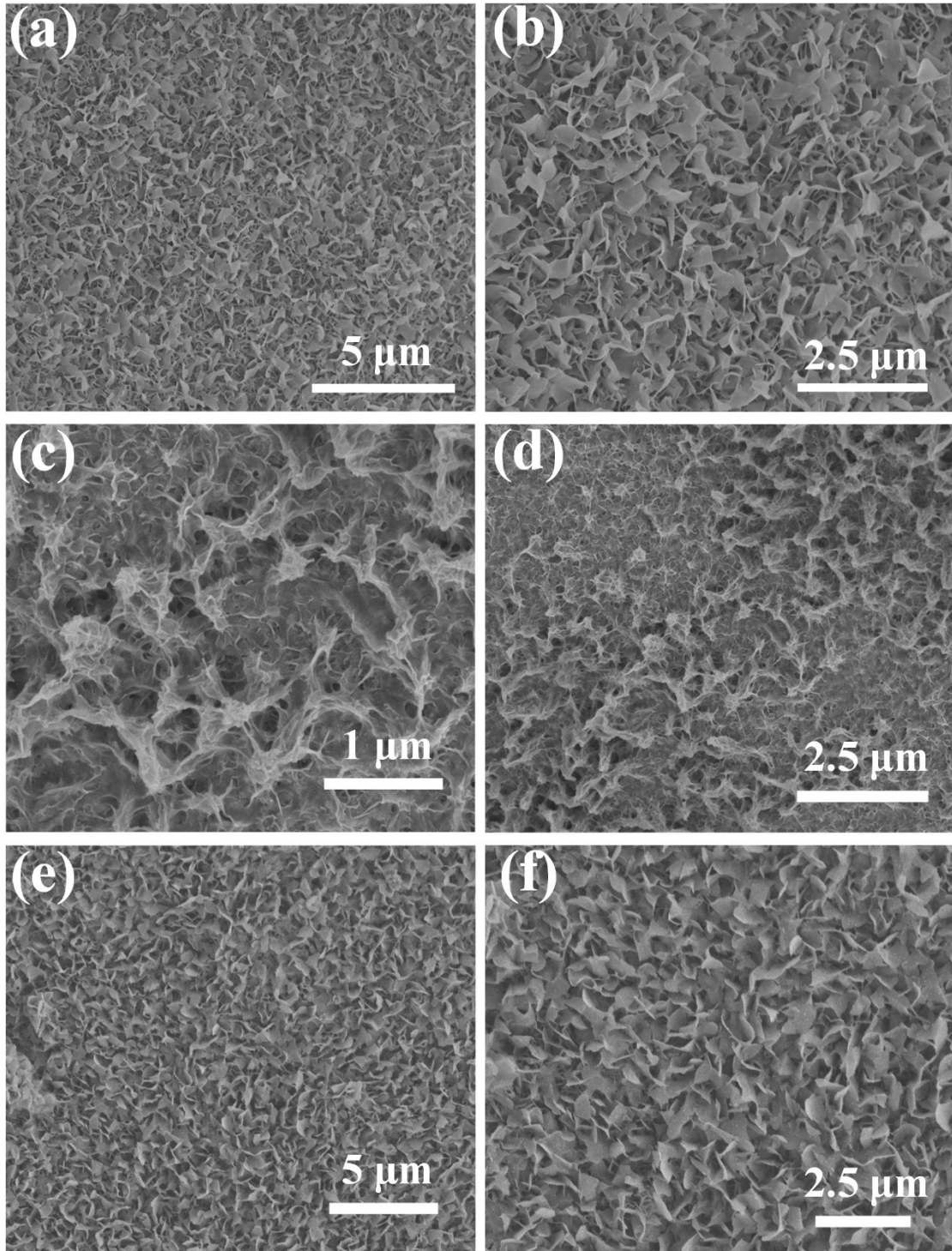


Figure S6. SEM images: (a, b) $\text{Co(OH)}_2/\text{Ni}_3\text{S}_2\text{-II}$, (c, d) $\text{Co(OH)}_2/\text{Ni}_3\text{S}_2\text{-I}$, (e, f) Co(OH)_2 .

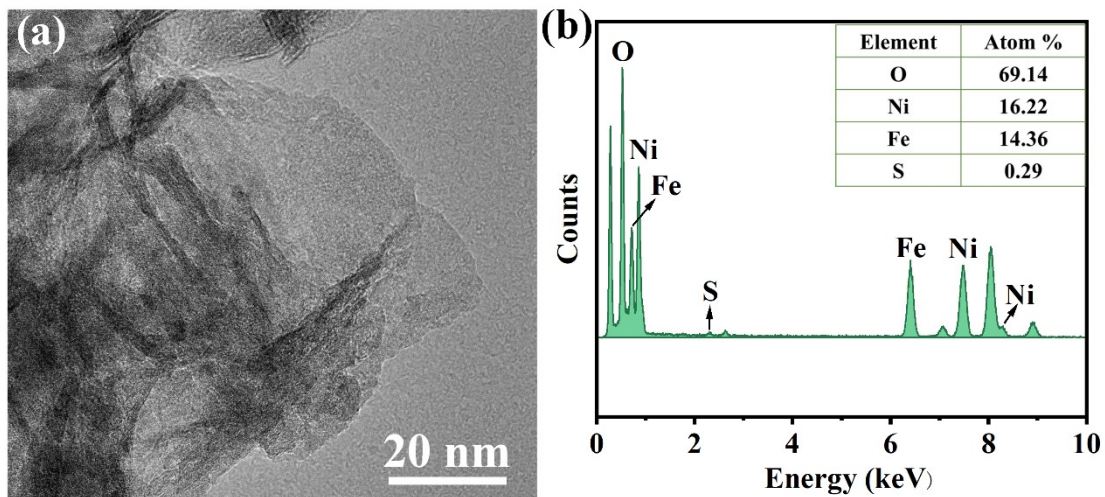


Figure S7. (a) TEM image of FeOOH/Ni₃S₂-II, (b) EDS spectrum of FeOOH/Ni₃S₂-II.

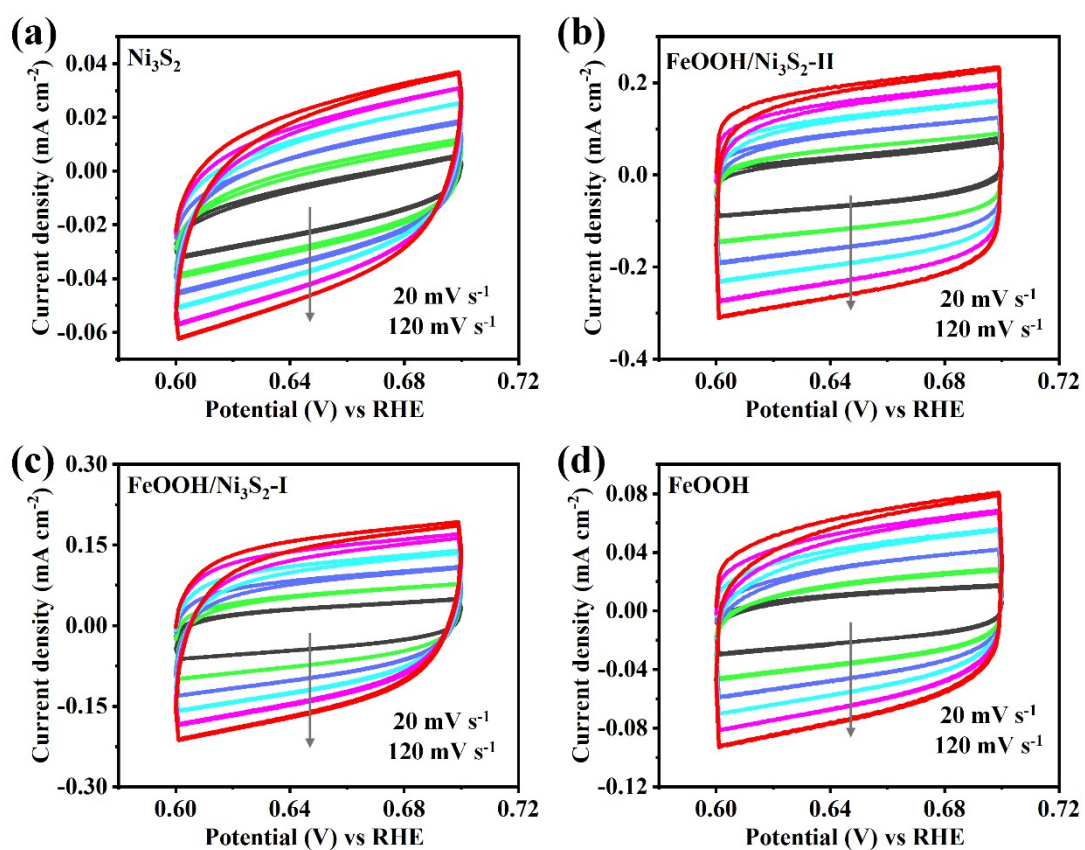


Figure S8. Cyclic voltammograms of (a) Ni₃S₂, (b) FeOOH/Ni₃S₂-II, (c) FeOOH/Ni₃S₂-I, (d) FeOOH.

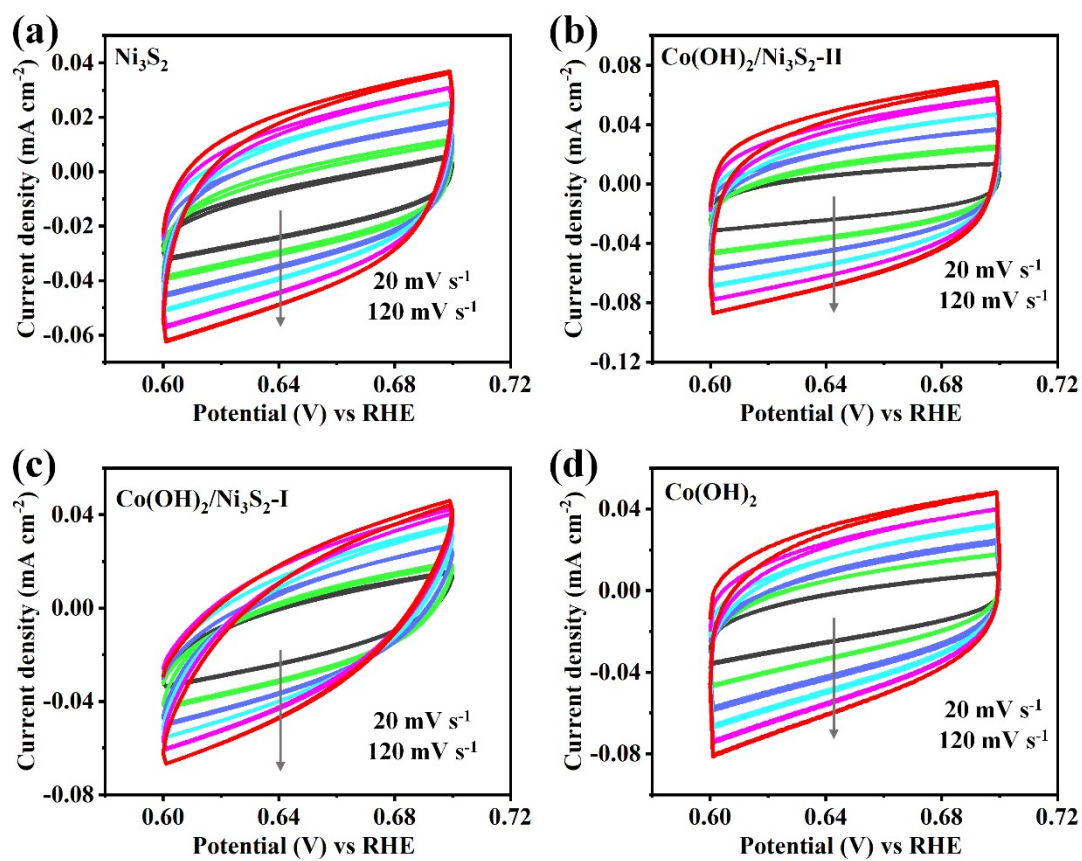


Figure S9. Cyclic voltammetry curves of (a) Ni_3S_2 , (b) $\text{Co(OH)}_2/\text{Ni}_3\text{S}_2\text{-II}$, (c) $\text{Co(OH)}_2/\text{Ni}_3\text{S}_2\text{-I}$, (d) Co(OH)_2 .

Table S1. Comparison of the OER performance of catalysts reported in literatures. (Current density: 100 mA cm⁻²).

Catalysts	Overpotential	Substrate	Reference
FeOOH/Ni ₃ S ₂ -II	269 mV	Ni foam	This work
Co(OH) ₂ /Ni ₃ S ₂ -II	348 mV	Ni foam	This work
FeOOH-Fe _{2.0}	263 mV	Ni foam	[1]
NiFe(OH) _x /FeS/IF	261 mV	Iron foam	[2]
Ni-FeOOH/NF	277 mV	Ni foam	[3]
FF-Na ₅₀₀ Ni ₅₀₀	212 mV	Fe Foam	[4]
FeNi(OH) _x /FeS/IF	273 mV	Iron foam	[5]
NiFe/NF	290 mV	Ni foam	[6]
2D Co ₃ O ₄	380 mV	Co powders	[7]
NiCo-OH	376 mV	Ni foam	[8]
Ni ₅ Co ₃ Mo-OH	304 mV	Ni foam	[8]
Ni-Co-S/CF	363 mV	Cu foam	[9]
Fe-Co-Ni hydroxide	319 mV	Ni foam	[10]

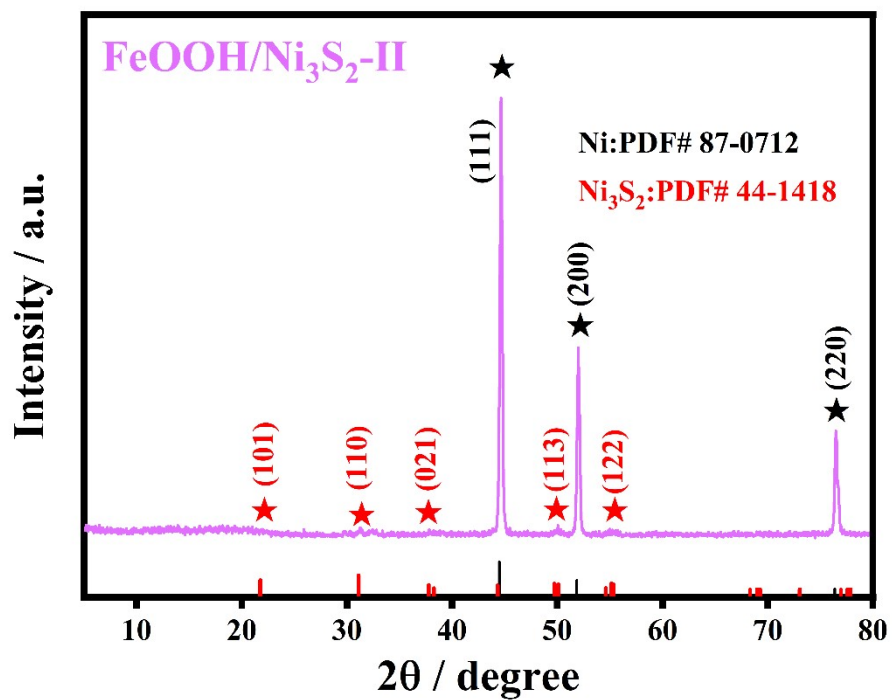


Figure S10. The XRD image after the OER of FeOOH/Ni₃S₂-II.

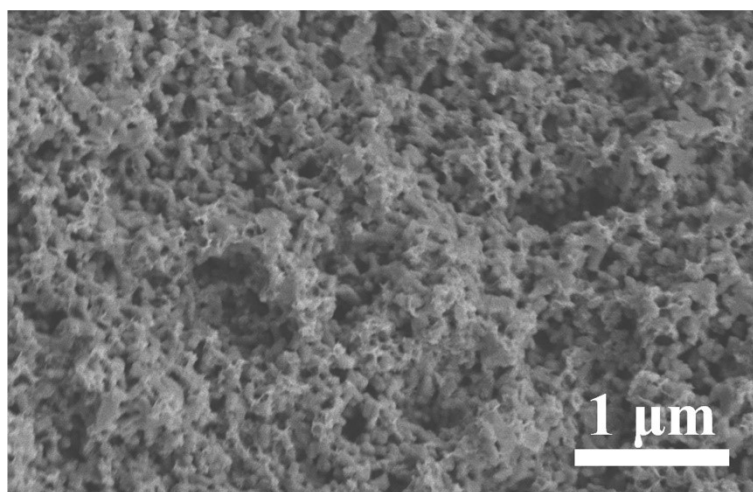


Figure S11. The SEM image after the OER of FeOOH/Ni₃S₂-II.

References

1. C. Ke, Q. Zhao, Y. Zhang, X. Yang and W. Xiao, *J. Alloy. Compd.*, 2023, **955**, 170131.
2. S. Niu, W.-J. Jiang, T. Tang, L.-P. Yuan, H. Luo and J.-S. Hu, *Adv. Funct. Mater.*, 2019, **29**, 1902180.
3. L. Li, Z. Wang, X. She, L. Pan, C. Xi, D. Wang, J. Yi and J. Yang, *J. Colloid Interface Sci.*, 2023, **652**, 789-797.
4. X. Liu, M. Gong, D. Xiao, S. Deng, J. Liang, T. Zhao, Y. Lu, T. Shen, J. Zhang and D. Wang, *Small*, 2020, **16**, 2000663.
5. Q.-W. Chen, X.-Y. Zhang, Y.-W. Dong, B.-Y. Guo, Y. Ma, L. Wang, R.-Q. Lv, Y.-L. Zhou, Y.-M. Chai and B. Dong, *J. Alloy. Compd.*, 2020, **835**, 155298.
6. H. Deng, H. Feng, G. Luo, R. Tu, Y. Zheng and Q. Shen, *Mater. Lett.*, 2022, **316**, 131999.
7. Y. Kang, H. Xie, D. Liu, M. Gao, P. K. Chu, S. Ramakrishna and X.-F. Yu, *Chem. Commun.*, 2019, **55**, 11406-11409.
8. S. Y. Hao, L. C. Chen, C. L. Yu, B. Yang, Z. J. Li, Y. Hou, L. C. Lei and X. W. Zhang, *ACS Energy Lett.*, 2019, **4**, 952-959.
9. T. Liu, X. Sun, A. M. Asiri and Y. He, *Int. J. Hydrog. Energy*, 2016, **41**, 7264-7269.
10. Q. L. Liu, H. Zhang, J. Xu, L. Z. Wei, Q. C. Liu and X. K. Kong, *Inorg. Chem.*, 2018, **57**, 15610-15617.